Titre: Title: A simple high-speed random number generator with minimal post-processing using a random Raman fiber laser

Auteurs: Authors: Frédéric Monet, Jean-Sébastien Boisvert, & Raman Kashyap

Date: 2021

Type: Article de revue / Article

Référence: Citation: Monet, F., Boisvert, J.-S., & Kashyap, R. (2021). A simple high-speed random number generator with minimal post-processing using a random Raman fiber laser. Scientific Reports, 11(1), 13182 (8 pages). https://doi.org/10.1038/s41598-021-92668-0

Titre de la revue: Journal Title: Scientific Reports (vol. 11, no. 1)

Maison d'édition: Publisher: Springer Nature

URL officiel: Official URL: https://doi.org/10.1038/s41598-021-92668-0

Supplementary Material

Random laser output power distributions at different pump powers

As pump power increases, the probability density function (PDF) describing the output power statistics will change. Fig. S1 displays histograms of the random laser output power at different pumps, and the associated Lévy exponent α. At low pump powers, the random laser's emission will be in an initial Gaussian regime, with $\alpha \approx 2$, as shown in Fig. S1(a). The laser's output at that pump power is only amplified spontaneous emission, since we are below threshold. Near the threshold, the laser's statistics will shift to a Lévy-like distribution with $\alpha < 2$, characterised by an asymmetrical long tail towards the higher powers, seen in Fig. S1(b-c). When pump power further increases, as displayed in Fig. S1(d), the α exponent starts increasing again, as the PDF returns towards a Gaussian distribution. At high powers, the random laser's emission is almost perfectly Gaussian, as seen in Fig. S1(e-f), where $\alpha \approx 2$ again.

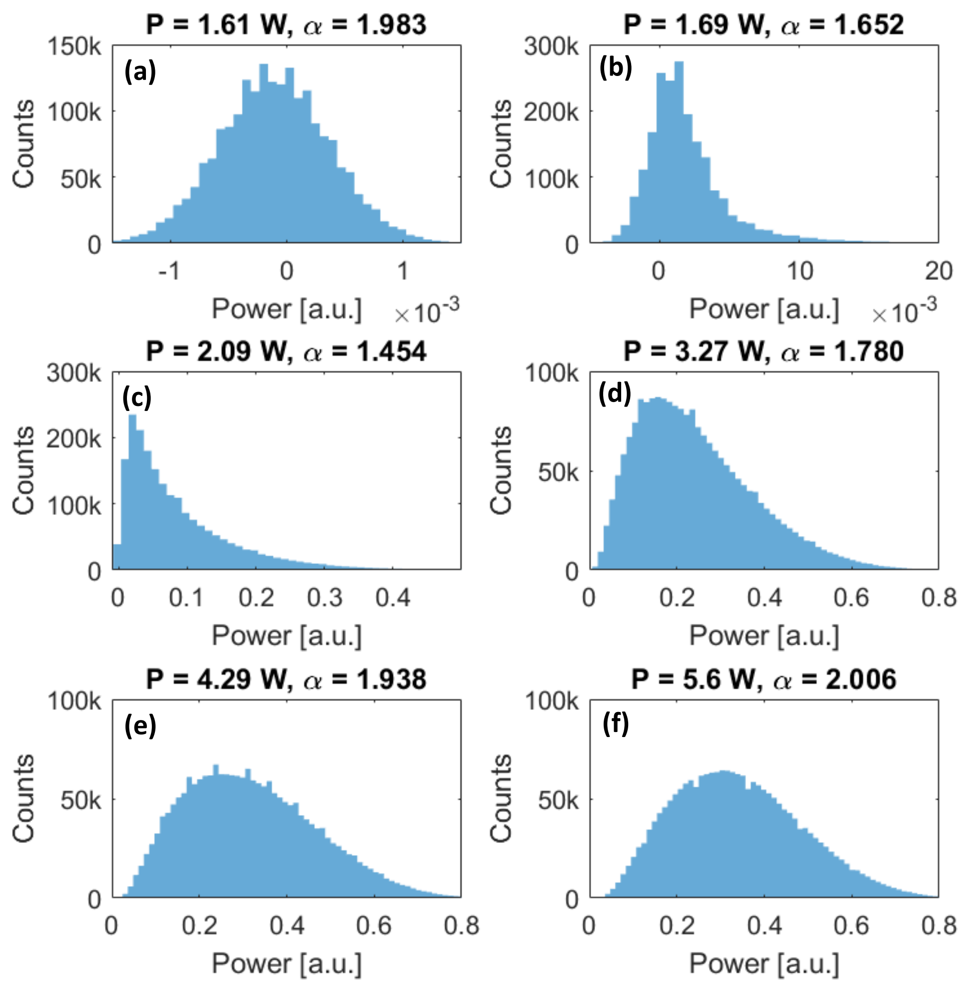

Fig. S1 Histograms of the output power at increasing pump powers. As pump power increases, the distribution is shown to shift from Gaussian (a), to Lévy-like distributions (b-d), with a return to Gaussian (e-f).

Spectrum of NZ-DS and TF optical fibers

In order to demonstrate the importance of pumping near the fiber's zero-dispersion wavelength (ZDW), the non-zero dispersion shifted (NZ-DS) optical fiber (SMF-LS, Corning) used for the cavity was replaced by 6 km of standard telecommunications fiber (TF) (SMF-28, Corning). The same fiber Bragg grating (FBG) was used in both experiments. While the TF's ZDW is around 1300 nm, the NZ-DS fiber's is near 1560 nm, which is much closer to the 1572 nm lasing wavelength, dictated by the FBG used in the experiment. Fig. S2 compares the spectrum of both lasers. As can be easily seen, in order to achieve the same linewidth broadening, a much higher pump power is necessary for the TF than for the NZ-DS fiber. This is not surprising, as the MI frequency is given by

$$\Omega_{MI} = \pm\sqrt{\frac{2\gamma P_0}{|\beta_2|}}, \quad \textbf{(S1)}$$

where γ is the fiber's nonlinearity, P_0 is the lasing power and β_2 is the fiber's group velocity dispersion parameter. Since in the case of the NZ-DS fiber, the lasing wavelength is near the ZDW, the β_2 parameter is much smaller than for the TF. As such, the same MI frequency can be obtained at lower pump powers.

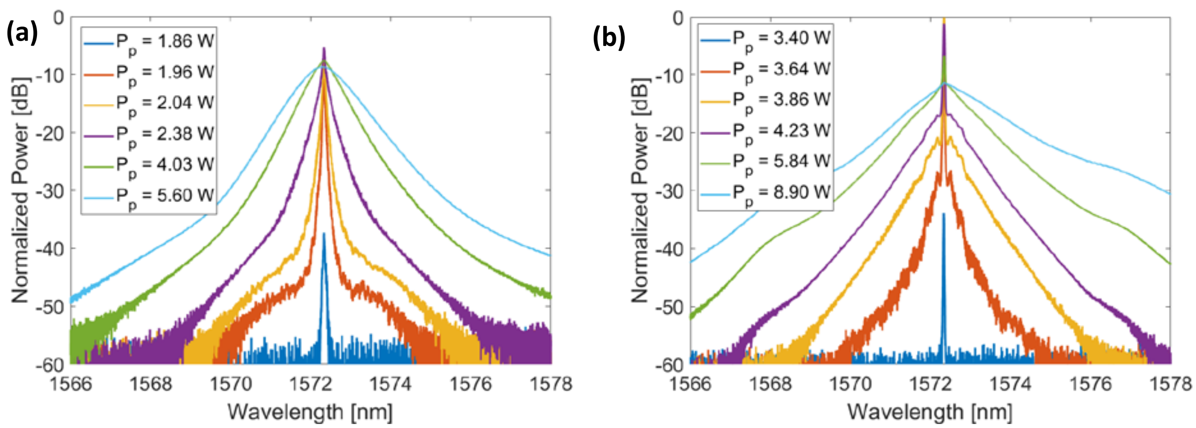

Fig. S2: Comparison of the spectrum when using (a) NZ-DS optical fiber and (b) standard telecommunication fiber.

Using Eq. (S1), and the specifications of telecommunications fiber SMF28 (β_2 = -25.3 ps^2/km, γ = 0.78 W/km), and an output power P_0 of 1 W, the theoretical modulation instability frequency is 2.52×10^{11} rad/s, which corresponds to a wavelength detuning of 0.33 nm at 1572 nm. This is in line with the observed side-lobes of Fig. S2(b). For the SMF-LS fiber (β_2 = -1.58 ps^2/km), the side-lobes are expected to appear near ±1.3 nm. Due to the important broadening of the laser, those side-lobes are challenging to observe. However, at the lowest pump powers, a symmetrical broadening can be observed at the calculated MI wavelengths, suggesting the presence of MI.